**TABLE 1 Experimental Results**

| Radar Technique | Microwave Band | Stimulus | Radar-Measured Frequency (Hz) | Piez. Sensor-Measured Frequency (Hz) | Radar-Measured Amplitude (mm) | Piez. Sensor-Measured Amplitude (mm) |
|---|---|---|---|---|---|---|
| CWSF | 6 GHz | Vibrodyne | 1.53 | 1.47 | 2.74 | 1.44 |
| CWSF | 6 GHz | Wind | 1.37 | 1.45 | 0.232 | 0.574 |
| CWMF | 5.5–6 GHz | Vibrodyne | 1.45 | 1.47 | 2.73 | 2.01 |
| CWMF | 5.5–6 GHz | Vibrodyne | 1.45 | 1.46 | 2.23 | 2.18 |

The method described above is able to separate the contributions of a set of targets, provided that vibration frequency is known. This can be adequately measured by calculating the FFT of the angle of the measured response in time, normalized with respect to the instantaneous microwave frequency.

## EXPERIMENTAL RESULTS

The radar technique has been tested at a facility of the Department of Civil and Environmental Engineering at the University of Perugia. The test structure was a vertical steel frame 10-m in height. A mechanical vibrodyne was positioned on the summit (Fig. 3). The CW radar was a prototype based on a network analyzer (HP 8753D) that operated as a coherent microwave transmitter and receiver, with a couple of horn antennas as described in [5]. The radar system was positioned in front of the structure, at a distance of 8 m. An accelerometer was installed on the structure at a height of 6 m.

CWSF measurement was carried out both with the structure artificially shaken by the vibrodyne, and naturally stirred by a light breeze. Figure 4 shows the FFT plots of the radar angular response in time with the structure naturally stirred. CWMF measurement was carried out with the structure artificially shaken. Figure 5 shows the plot of the expression in Eq. (2). Table 1 summarizes the results of the radar measurements and compares them to the reference data obtained with the accelerometer installed on the structure.

The agreement between CWSF tests and accelerometer measurements is rather qualitative. In effect, as the radar performs a global displacement measurement, the comparison with a punctual sensor is of minor significance.

On the contrary, because the CWMF technique is able to separate the contribution of the structure section where the accelerometer was installed, the agreement between CWMF tests and accelerometer measurements is more satisfactory.

## CONCLUSION

The non-contact remote operating microwave techniques described in this paper provided effective measurements of the dynamic response of large structures. Furthermore, it has been demonstrated that the CWSF technique is able to measure the response of vertical structures without artificial stimuli.


## ACKNOWLEDGEMENTS

This work was partially supported by the Winderful Project (Project of National Interest 2001) funded by the Italian Ministry of Research. The authors are grateful to Marco Breccolotti for his technical support during the measurement campaign.


## REFERENCES


1. S.W. Doebling, C.R. Farrar, M.B. Prime, and D.W. Shevitz, Damage identification and health monitoring of structural and mechanical systems from change in their vibration characteristics: A literature review, Los Alamos National Laboratory Report LA-13070-MS, 1996, available at http://lib-www.lanl.gov
2. G. Hearn and R.B. Testa, Modal analysis for damage detection in structures, J Structural Eng 117 (1991), 3042–3063.
3. E.P. Tomasini (Ed.), Special issues on advances and application in vibration measurement by laser techniques, Optics Lasers Eng 38 (2002).
4. C.R. Farrar, T.W. Darling, A. Migliorini, and W.E. Baker, Microwave interferometer for non-contact vibration measurements on large structures, Mechanical Sys Signal Processing 13 (1999), 241–253.
5. M. Pieraccini, G. Luzi, and C. Atzeni, Terrain mapping by ground-based interferometric radar, IEEE Trans Geosci Remote Sensing 39 (2001), 2176–2181.




# A ROBUST AND EFFICIENT METHOD FOR OBTAINING THE COMPLEX MODES IN INHOMOGENEOUSLY FILLED WAVEGUIDES


**Juan A. Monsoriu,[1] Angela Coves,[2] Benito Gimeno,[3] Miguel V. Andres,[3] and Enrique Silvestre[4]**

[1] Departamento de Física Aplicada
Universidad Politécnica de Valencia
E-46022 Valencia, Spain
[2] Departamento de Física y Arquitectura de los Computadores
Universidad Miguel Hernández de Elche
E-03300 Orihuela, Spain
[3] Departamento de Física Aplicada
ICMUV
E-46100 Burjassot, Spain
[4] Departamento de Óptica
Universidad de Valencia
E-46100 Burjassot, Spain


*Received 24 October 2002*


**ABSTRACT:** *In this paper, we present a computational simulation of the complex wave propagation in inhomogeneously filled waveguides with lossless and lossy dielectrics. We use a biorthonormal-basis method as a numerical technique. The behavior of complex modes in different waveguides whose characterization with other methods involves some difficulties is analyzed.* © 2003 Wiley Periodicals, Inc. Microwave Opt Technol Lett 37: 218–222, 2003; Published online in Wiley InterScience (www.interscience.wiley.com). DOI 10.1002/mop.10875


**Key words:** *dielectric waveguides; complex modes; image guide; Galerkin method*

## 1. INTRODUCTION

Complex modes in lossless waveguides are guided waves with complex propagation constants. Due to the lossless nature of the structure supporting such modes, they always exist in pairs with complex conjugate propagation constants of opposite sign, so that

both have the same attenuation constant [1]. Each one of these complex modes has a total power flow equal to zero, with one sign inside the dielectric region and the opposite sign outside. For the corresponding conjugate mode, these signs are the opposite ones. Complex modes in a circular waveguide containing a coaxial dielectric rod were first predicted in [2] and experimental results were reported in [3]. Investigations have shown that the complex waves have to be included in the field expansion used in field matching procedures for the analysis of discontinuity problems in cylindrical dielectric-loaded waveguides [4], cylindrical resonators [5], and other waveguide structures, such as finlines [6] or shielded microstrips [7]. Their omission leads to erroneous results. Complex modes in a shielded rectangular dielectric image guide, which can be considered as a rectangular waveguide with a rectangular dielectric insert, have been studied, for instance, in [8, 9].

Because complex waves constitute an unavoidable part of the spectrum of the operator describing electromagnetic field propagation in inhomogeneously dielectric-filled waveguides, it is important to have a robust method of analysis in order to deal with these modes to ensure accurate and efficient computational modelling. However, the characterization of complex modes with conventional methods, such as FDTD [9], presents some difficulties (the nature of complex modes makes their detection difficult, while other propagating modes could mask them). In this paper we present numerical calculations of the spectra of shielded dielectric image guides and dielectric-loaded cylindrical waveguides—showing their dependence on frequency, their power transmission, and their behavior in presence of losses—by using our biorthonormal-basis method [10, 11]. It is a straightforward and spurious mode-free method that is able to obtain the complex modal spectrum in inhomogeneously filled waveguides with lossy dielectric of arbitrary profiles. The key is to transform the differential vector wave equations into a linear matrix eigenvalue problem by means of the Galerkin procedure. From a computational point of view this method is very efficient, because the integrals involved in the matrix elements are, in general, frequency independent; thus they have to be evaluated only once to obtain the dispersion curves. The present method has been successfully applied to the analysis of rectangular waveguides filled with dielectric slabs [11], and open guides as optical fibers [10]. Comparisons between numerical results for ordinary and complex propagation in inhomogeneous cylindrical and rectangular waveguides show excellent agreement with existing data available in the literature, which indicates the capability of the presented technique.

## 2. THEORETICAL FORMULATION

Guided modes in an inhomogeneously dielectric-filled waveguide, which are uniform in the propagation direction $z$, characterized by a complex relative dielectric permitivity $\varepsilon_r(x, y)$, and with no magnetic properties $\mu = \mu_0$, verify a set of dimensionally reduced differential equations exclusively involving the transverse coordinates $x$ and $y$. We obtain this set of equations from Maxwell's equations by assuming that the electromagnetic field possess a harmonic dependence $e^{j\omega t - \gamma z}$ with $\gamma$ the modal propagation constant ($\gamma = \alpha + j\beta$) and $\omega$ the angular frequency. In terms of the transverse components of the magnetic and electric fields, $\boldsymbol{h}_t = (h_x, h_y)$ and $\boldsymbol{e}_t = (e_x, e_y)$, these equations can be rewritten as [11]:

$$L\boldsymbol{h}_t = -\gamma^2 \boldsymbol{h}_t, \quad L^\dagger \bar{\boldsymbol{e}}_t = -\gamma^{*2} \bar{\boldsymbol{e}}_t, \tag{1}$$

where $\bar{\boldsymbol{e}}_t = (e_y^*, -e_x^*)$, $L^\dagger$ is the adjoint operator of $L$, and * denotes the complex-conjugate operation. The most relevant property of the above equations is that they constitute a system of eigenvalues equations for the $L$ operator and its adjoint $L^\dagger$. Because $\boldsymbol{h}_t$ and $\bar{\boldsymbol{e}}_t$ are the eigenfunctions of the $L$ and $L^\dagger$ operators, respectively, they are closely related. In fact, they verify what is called the "biorthogonality" relationship, $\langle \bar{\boldsymbol{e}}_{t(n)}, \boldsymbol{h}_{t(m)} \rangle = \delta_{nm}$. Despite its apparently formal character, this relation has a very clear physical meaning if we rewrite the inner product in its integral form

$$\langle \bar{\boldsymbol{e}}_{t(n)}, \boldsymbol{h}_{t(m)} \rangle \equiv \int_S \bar{\boldsymbol{e}}^*_{t(n)} \cdot \boldsymbol{h}_{t(m)} dS \equiv \int_S (\boldsymbol{e}_{t(n)} \times \boldsymbol{h}_{t(m)}) \hat{\boldsymbol{z}} dS = \delta_{nm}, \tag{2}$$

where $\hat{\boldsymbol{z}}$ represents the unitary vector along the $z$ direction, and $S$ is the cross section of the waveguide. In the above equation, we can recognize the biorthogonality relation as the well-known "orthogonality" relationship that is satisfied by all the modes in conventional closed waveguides, that is, both the noncomplex [12] and complex [1, 4] ones.

The key of this method is to obtain a matrix representation of the vector wave in Eq. (1) on a basis that is defined by the modes of an auxiliary system. The biorthogonality relationship allows us to obtain efficiently the coefficients of the modal expansions in terms of the eigenvectors as well as the propagation constants by means of the eigenvalues. Once a matrix representation is provided, we shall obtain the whole spectrum (or a subset) of the guided modes of the system by means of the numerical diagonalization of such operator matrix representation using a standard iterative technique.

With this aim, we need an appropriate auxiliary system characterized by a permitivity $\tilde{\varepsilon}(x, y)$ (with the same boundary conditions as the waveguide problem) that provides the auxiliary basis

$$\tilde{L}\tilde{\boldsymbol{h}}_t = -\tilde{\gamma}^2 \tilde{\boldsymbol{h}}_t, \quad \tilde{L}^\dagger \bar{\tilde{\boldsymbol{e}}}_t = -\tilde{\gamma}^{*2} \bar{\tilde{\boldsymbol{e}}}_t. \tag{3}$$

Hence, the eigenvectors of $\tilde{L}$ and $\tilde{L}^\dagger$ satisfy the biorthogonality relation $\langle \bar{\tilde{\boldsymbol{e}}}_{t(n)}, \tilde{\boldsymbol{h}}_{t(m)} \rangle = \delta_{nm}$. By breaking down the problem under consideration to $L = \tilde{L} + \Delta$, and expanding the eigenvectors of $L$ and $L^\dagger$ in terms of the auxiliary eigenvectors, we can represent the vector wave in Eq. (1) in a matrix form. Each element, $L_{ij}$ of the matrix can be calculated by means of the expansion

$$L_{ij} = \langle \bar{\tilde{\boldsymbol{e}}}_{t(i)}, L\tilde{\boldsymbol{h}}_{t(j)} \rangle = -\tilde{\gamma}_i^2 \delta_{ij} + \langle \bar{\tilde{\boldsymbol{e}}}_{t(i)}, \Delta\tilde{\boldsymbol{h}}_{t(j)} \rangle, \tag{4}$$

and its diagonalization provides the eigenvalues $-\gamma^2$ and the eigenvectors $\boldsymbol{h}_t$, that is, the propagation constants and transverse magnetic amplitudes of the modes. Then both the axial component of the magnetic field and the transverse and axial components of the electric field can be calculated from $\boldsymbol{h}_t$ through constraints given by Maxwell's equations [12].

The present formulation is valid for the general case of waveguides with arbitrarily shaped cross section and arbitrary inhomogeneity of the dielectric-filling medium. In this work, we have applied this case to investigate the complex spectrum of dielectric-slab-loaded rectangular waveguides and dielectric-rod-loaded circular waveguides. As an auxiliary system, we have chosen a homogeneously filled rectangular waveguide in the first case, and a cylindrical one in the second case, whose modes are analytically known [12, 13]. Under these considerations, the matrix given by Eq. (4) is real and nonsymmetric when the waveguide problem is filled with a lossless medium—with $\varepsilon_r(x, y)$ a real function—so that its eigenvalues $-\gamma^2$ are either real or complex conjugate pairs, because they are zeros of a polynomial with real coefficients. Complex conjugate pairs of $\gamma^2$ characterize the so-

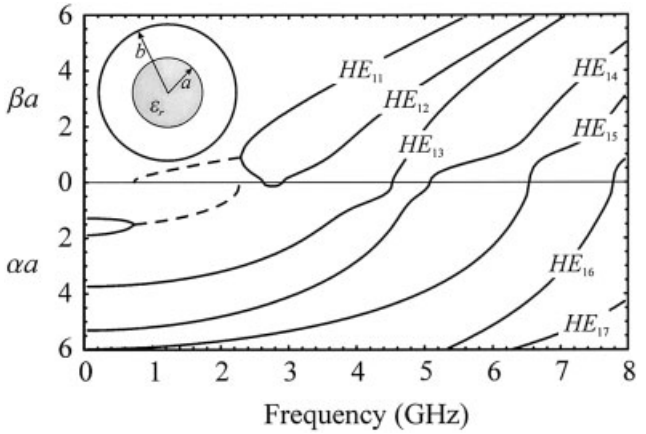


**Figure 1** Normalized propagation constant of the first $HE_{1m}$ modes in a dielectric-rod-loaded waveguide ($a = 8.99$ mm, $b = 12.7$ mm, and $\varepsilon_r = 37$) vs. frequency

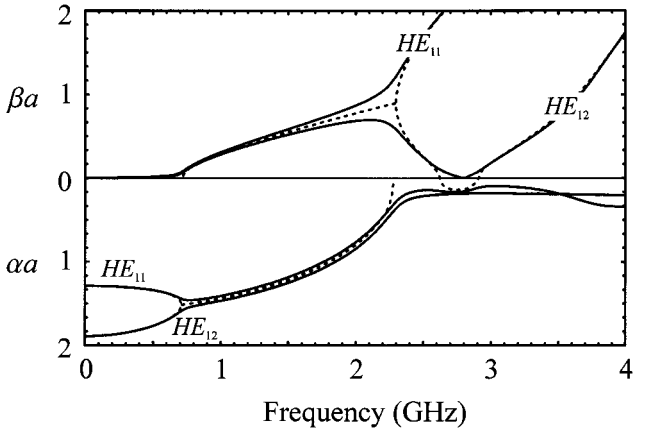


**Figure 2** Behavior of the complex modes $HE_{11}$-$HE_{12}$ shown in Fig. 1(a) with (solid curve) and without (dotted curve) losses ($\tan\delta = 0.04$)

called complex modes. When the waveguide is filled with lossy dielectrics—with $\varepsilon_r(x, y)$ a complex function—the matrix of Eq. (4) is complex and nonhermitian, so that all the modes are complex and cease to be conjugates of each other.

### 3. NUMERICAL RESULTS

The present method was successfully applied in [11] to analyze standard dispersion behavior of rectangular waveguides loaded with lossless dielectrics of low permittivity. We will now focus on complex propagation in closed waveguides of different geometry loaded with moderate and high permittivity dielectrics.

The first case is an inhomogeneously filled cylindrical waveguide of radius $b = 12.7$ mm, axially loaded with a concentric dielectric rod of radius $a = 8.99$ mm and relative permittivity $\varepsilon_r = 37$ (see Fig. 1). This case is particularly interesting because an analytical solution does exist [4, 14]. The electromagnetic fields that can exist within this structure are both transversal ($TE_{0m}$ and $TM_{0m}$) and hybrid modes ($HE_{nm}$, $n \neq 0$). To solve this case, we have taken the normalized vector mode functions of an empty cylindrical guide (written in terms of Bessel functions) [13] as the auxiliary basis functions. The choice of this auxiliary system permits an analytical evaluation of the elements of the matrix that represents the $L$ operator. Thus, the precision of the method will be determined by the number of auxiliary modes used for the expansion of the fields.

We consider separately each azimuthal order $n$, since the coupling between modes of different azimuthal order is zero. We have not obtained any complex mode in this waveguide without azimuthal dependence ($TE_{0m}$ and $TM_{0m}$ modes), thus confirming what has been previously achieved in [1] by using a different approach. Next, we present the particular case of the hybrid modes with $n = 1$, $HE_{1m}$. In Table 1 we compare our results with the analytical solution obtained by solving the characteristic equation for the propagation constants [4, 14] for working frequencies at 2 GHz and 6 GHz. We can see that, for the first hybrid modes, the relative error is smaller than 0.01% when only 100 auxiliary modes are used to expand the fields. It only takes 1 s to solve each azimuthal order using a Silicon Graphics Origin-2000 machine.

In Figure 1, we present the complex dispersion curves for the first hybrid modes $HE_{1m}$, also obtaining very good agreement with previous results [4]. In this figure, the propagation constants are plotted vs. frequency. The solid curve is either the normalized real attenuation constant $\alpha a$ or the normalized imaginary propagation constant $\beta a$. The dashed curves are the complex propagation constant $\gamma a$. Complex propagation occurs in the frequency ranges 0.74 GHz $\leq f \leq$ 2.29 GHz for the hybrid modes $HE_{11}$-$HE_{12}$. Next, we show the effect of the losses in the dielectric rod ($\tan\delta = 0.04$) in the dispersion curves of the complex modes. In Figure 2, the normalized propagation constant is plotted as a function of the frequency for the $HE_{11}$ and $HE_{12}$ modes. The corresponding "lossless" waves are shown with dotted lines for comparison. The conjugate complex modes appear at frequency of 0.74 GHz as a combination of the evanescent $HE_{11}$ and $HE_{12}$ modes and exist up to 2.29 GHz, before giving way to the propagating-$HE_{11}$ and backward-$HE_{12}$ modes. In the presence of losses these bifurcations disappear, and the two complex modes are not conjugate of each other, thus their degeneracy is broken.

**TABLE 1 Normalized Propagation Constants for $HE_{1m}$ Modes of a Circular Guide with a Dielectric Rod ($a = 8.99$ mm, $b = 12.7$ mm, $\varepsilon_r = 37$)**

| | | Analytical Solution [6, 31] | | Present Method | | |
|---|---|---|---|---|---|---|
| Frec. (GHz) | Mode | $\beta a$ | $\alpha a$ | $\beta a$ | $\alpha a$ | Relative Error (%) |
| 2 | $HE_{11}$-$HE_{12}$ | 0.776367 | 0.800281 | 0.776365 | 0.800283 | 0.0002 |
| | $HE_{13}$ | — | 3.202981 | — | 3.202952 | 0.0009 |
| | $HE_{14}$ | — | 4.816328 | — | 4.816231 | 0.0020 |
| | $HE_{15}$ | — | 5.694747 | — | 5.694650 | 0.0031 |
| 6 | $HE_{11}$ | 6.410728 | — | 6.410742 | — | 0.0002 |
| | $HE_{12}$ | 5.067247 | — | 5.067325 | — | 0.0015 |
| | $HE_{13}$ | 4.186134 | — | 4.186489 | — | 0.0085 |
| | $HE_{14}$ | 0.900286 | — | 0.900371 | — | 0.0094 |
| | $HE_{15}$ | — | 2.283621 | — | 2.283385 | 0.0103 |

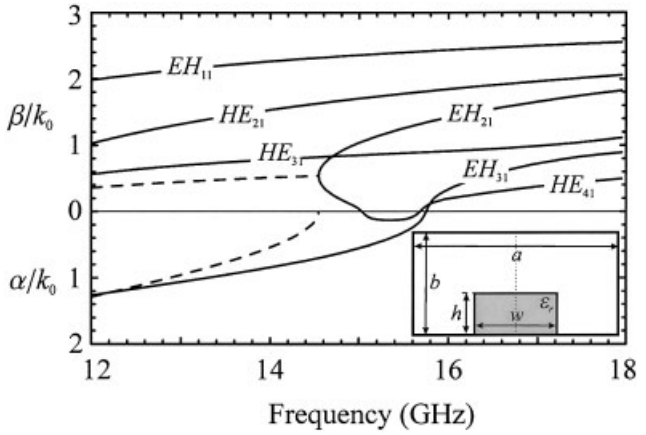


**Figure 3** Normalized propagation constant vs. frequency in a the image guide with $a = 15.789$ mm, $b = 7.899$ mm, $w = 6.9$ mm, $h = 3.2$ mm, and $\varepsilon_r = 9$

The second modeled system (see Fig. 3) is a dielectric image guide shielded with a standard rectangular waveguide. This kind of structure is widely used in the design of devices in the millimeter-wave frequency range. We have taken the vector-mode functions of an empty rectangular guide as the auxiliary basis system [13]. Again, we will focus on complex propagation in this image guide. The modes of propagation of such waveguides are not *TM* or *TE* modes, but hybrid modes, for which the designation of [15] is used. In Figure 3, we present the normalized propagation constant vs. the frequency ($k_0$ represents the free-space wave number) for the first six modes, including complex modes (dashed lines), for a dielectric shielded image guide with parameters $a = 15.789$ mm, $b = 7.899$ mm, $w = 6.9$ mm, $h = 3.2$ mm, and $\varepsilon_r = 9$. Complex propagation occurs below a frequency of 14.57 GHz, then gives way to the propagating-$EH_{12}$ and backward-$HE_{41}$ modes. This behavior is similar to that described for the complex conjugated modes $HE_{11}$-$HE_{12}$ in an inhomogeneously filled cylindrical waveguide (Figs. 1 and 2).

The number of basis functions employed in this system is 2000, and the computation time required is 58 s per frequency point on a Silicon Graphics Origin-2000 machine. We found very good agreement with similar results presented by Strube and Ardnt [8], confirming the efficiency of our method compared to other techniques [9].

In addition to the propagation constants, the present method can provide the field patterns of the modes, including complex modes. Using these fields we can obtain the power flow for these modes. As an example, in Figure 4 we show the real part of the Poynting vector ($z$ component) for one of the complex conjugate modes shown in Figure 3 at 14 GHz. It is negative in the dielectric region and positive outside, and vice versa for the other one, with the total power transmitted by each complex mode through the total cross section of the shielded dielectric image-guide equal to zero. For comparison, we have also plotted the power distribution of the propagative $EH_{11}$, $HE_{21}$, and $HE_{31}$ modes at the same frequency. The total transmitted power is now different from zero, being positive for the three propagative modes. The $EH_{11}$ and $HE_{21}$ modes focus the energy inside the dielectric region, whereas the energy is distributed outside the dielectric region for the $HE_{31}$ mode. A similar result is presented in [16] with other structural parameters for the first two propagative modes using the finite-element method.

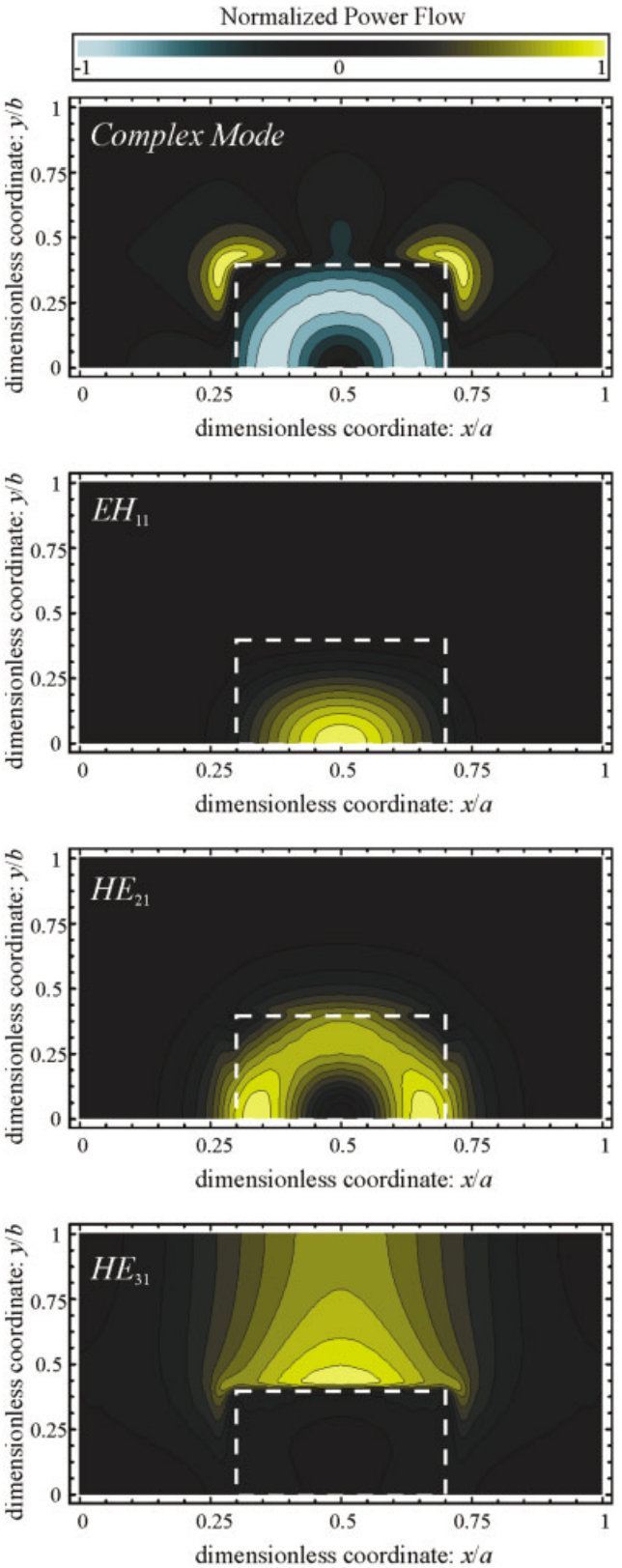


**Figure 4** Real part of the Poynting vector ($z$ component) for the complex mode and propagative $EH_{11}$, $HE_{21}$, and $HE_{31}$ modes shown in Fig. 3 at 14 GHz. [Color figure can be viewed in the online issue, which is available at www.interscience.wiley.com.]

## 4. CONCLUSION

In this paper, the biorthonormal-basis method has been used to model the complex wave-propagation constant and the transverse-field pattern in inhomogeneously filled waveguides with lossless and lossy dielectrics. The differential operator governing the transverse fields is transformed into a linear-matrix eigenvalue problem, using the eigenvectors of an auxiliary problem to expand the modes of the original problem. This method has been applied to the calculation of the complex modes in dielectric-rod-loaded circular waveguides and dielectric-slab-loaded rectangular waveguides, which provides an example demonstrating the capability of the method to include the dielectric losses directly in its formulation. The method is free of spurious modes and, in most cases (as in the systems shown in this paper), the integrals involved in the matrix elements can be obtained analytically, and the only numerical approximation is the finite number of modes used for the expansion of the fields. The high accuracy necessary to obtain complex modes is fully achieved by our method. On the contrary, other methods involve serious difficulties.


## ACKNOWLEDGEMENT

This work was financially supported by the Ministerio de Ciencia y Tecnología (grant TIC2000-0591-C03-03), Spain.


## REFERENCES


1. A.S. Omar and K.F. Schünemann, Complex and backward-wave modes in inhomogeneouly and anisotropically filled waveguides, IEEE Trans Microwave Theory Techn MTT-35 (1987), 268–274.
2. P.J.B. Clarricoats and B.C. Taylor, Evanescent and propagating modes in dielectric loaded circular waveguide, Proc Inst Elec Eng 111 (1964), 1951–1956.
3. V.A. Kalmyk, S.B. Rayevskiy, and V.P. Ygvyumov, An Experimental verification of existence of complex waves in a two-layer, circular, shielded waveguide, Radio Eng Electron Phys 23 (1978), 17–19.
4. K.A. Zaki, S. Chen, and C. Chen, Modelling discontinuities in dielectric-loaded waveguides, IEEE Trans Microwave Theory Techn 36 (1988), 1804–1810.
5. C. Chen and K.A. Zaki, Resonant frequencies of dielectric resonators containing guided complex modes, IEEE Trans Microwave Theory Techn 36 (1988), 1455–1457.
6. T. Rozzi, L. Pierantoni, and M. Farina, Eigenvalue approach to the efficient determination of the hybrid and complex spectrum of inhomogeneously closed waveguide, IEEE Trans Microwave Theory Techn 45 (1997), 345–353.
7. W. Huang and T. Itoh, Complex modes in lossless shielded microstrip lines, IEEE Trans Microwave Theory Techn 36 (1988), 163–164.
8. J. Strube and F. Arndt, Rigorous hybrid-mode analysis of the transition from rectangular waveguide to shielded dielectric image guide, IEEE Trans Microwave Theory Techn MTT-33 (1985), 391–401.
9. M.A. Hernández-López and M. Quintillan, Propagation characteristics of modes in some rectangular waveguides using the finite-difference time-domain method, J Electromagn Waves Appl 14 (2000), 1707–1722.
10. E. Silvestre, M.V. Andrés, and P. Andrés, Biorthonormal-basis method for vector description of optical-fiber modes, J Lightwave Technol 16 (1998), 923–928.
11. E. Silvestre, M.A. Abian, B. Gimeno, A. Ferrando, M.V. Andrés, and V. Boria, Analysis of inhomogeneously filled waveguides using a biorthonormal-basis method, IEEE Trans Microwave Theory Techn 48 (2000), 589–596.
12. R.E. Collin, Field theory of guided waves, 2nd ed. IEEE Press, New York, 1991.
13. N. Marcuvitz, Waveguide handbook, Peter Peregrinus Ltd., London, 1986.
14. K.A. Zaki and A.E. Atia, Modes in dielectric-loaded waveguides and resonators, IEEE Trans Microwave Theory Techn MTT-31 (1983), 1039–1044.
15. K. Solbach and I. Wolff, The electromagnetic fields and the phase constants of dielectric image lines, IEEE Trans Microwave Theory Techn MTT-26 (1978), 266–274.
16. J.-F. Lee, D.-K. Sun, and Z.J. Cendes, Full-wave analysis of dielectric waveguides using tangential vector finite elements, IEEE Trans Microwave Theory Techn 39 (1991), 1262–1271.




# REDUCING RESONANT LENGTH OF SIDEWALL-INCLINED SLOTS IN A RECTANGULAR WAVEGUIDE


**Abbas Ali Heidari, Keyvan Forooraghi, and Mohammad Hakkak**
Department of Electrical Engineering
Tarbiat Modarres University
P.O. Box 14115-143, Tehran, Iran


*Received 19 October 2002*

**ABSTRACT:** *In this paper, the admittance characteristics of a dielectric filled inclined slot in the narrow wall of a rectangular waveguide have been calculated. By enforcing the continuity of the tangential magnetic field through the slot aperture, an integral equation with the tangential electric field in the slot as the unknown is obtained. An entire domain method of moments (MoM) is used to solve the integral equation. Numerical results show that the slot can resonate without penetrating onto the top and bottom broad walls of the waveguide. It has also been shown that the resonant frequency (length) and the resonant conductance of the slot depend on the dielectric constant of the material filling the slot. The computed results are shown to be in good agreement with those obtained by HP-HFSS.* © 2003 Wiley Periodicals, Inc.
Microwave Opt Technol Lett 37: 222–226, 2003; Published online in Wiley InterScience (www.interscience.wiley.com). DOI 10.1002/mop.10876

**Key words:** *narrow wall slot; dielectric filled slot*

## 1. INTRODUCTION

Inclined slots in the narrow wall of a rectangular waveguide, so-called edge slots, have been widely used in radars and satellite systems. These slots extend onto the broad walls of the waveguide to produce resonance, which complicates the analysis of narrow wall slots. Furthermore, fabrication of planar arrays become difficult, since metallic spacers should be placed in between the guides, which in turn increases the back radiation of the array.

A number of investigations have been reported on these slots [1–4]. In all these works, the edge slot is tilted to excite and penetrate the broad walls of the waveguide. Hashemi-Yeganeh and Elliott [5] analyzed untilted edge slots excited by tilted wires in a rectangular waveguide. One of the most important results they obtained in their study was the discovery of the possibility of a resonant condition between the slot and tilted wires, which does not require the slot to be continued onto the broad walls. This permits embedding an array of these composite elements in a ground plane. In their analysis it was assumed that the slot is embedded in an infinite ground plane. Hirokawa et al. [6] analyzed this structure by including the actual structure, using a spectrum of the two-dimensional solutions (S2DS) method [7]. Their results show that the effect of modelling the actual outer cross section of the waveguide, instead of assuming an infinite ground plane, is small. Actually, the difference is smaller than the measurement error in the experimental setup. Hirokawa and Kildal [8] proposed